

Frequency Domain System Identification When Assuming Unknown But Bounded Errors

Lee Barford
Integrated Solutions Laboratory
HPL-97-35
March, 1997

dynamical
systems
identification,
digital error,
set-membership
assumption,
non-linear
optimization

When performing parameter estimation of dynamical systems, one must evaluate unknown variables given uncertain measurements. Often the problem is approached using a probabilistic description of the uncertainty and statistical estimation theory is applied.

Another approach is to make the so-called "set-membership" or "unknown-but-bounded error" (UBBE) assumption. Here it is assumed that the measurements contain errors that are within known bounds.

This paper discusses the frequency domain system identification problem under the UBBE assumption. It demonstrates that the set of all possible identifications is a finite union of polyhedra. The paper also shows how the problem of finding one valid identification reduces to finding a feasible solution to a nonlinear system of equations under box constraints. An example of applying the resulting algorithm to actual measurements is given.

1 INTRODUCTION

When performing parameter estimation of dynamical systems, one must evaluate unknown variables given uncertain measurements. Often the problem is approached using a probabilistic description of the uncertainty and statistical estimation theory is applied.

Another approach is to make the so-called “set-membership” or “unknown-but-bounded error” (UBBE) assumption [1][2]. Under the UBBE assumption, it is assumed that the measurements contain errors that are within known bounds. That is, every time some quantity m is measured (yielding a measured value \hat{m}), it is assumed that a lower bound \underline{m} and upper bound \bar{m} can be computed from \hat{m} such that the true value of the quantity is contained in the bounds: $\underline{m} \leq m \leq \bar{m}$.

There are several ways the bounds can be created. The bounds can come from manufacturers’ specifications. They can be the expanded uncertainty resulting from a metrological analysis of the measurement equipment [3]. Approximate bounds can be obtained by taking the extremal values from a set of repeated measurements.

The UBBE assumption may be more reasonable than a probabilistic description of measurement error for a measurement where digitization error dominates environmental noise. An audio-frequency filter characterization measurement (Fig. 1) provides an example. A data acquisition board was used with one digital-to-analog (D/A) converter and two analog-to-digital (A/D) converters, all triggered simultaneously from the same clock. The D/A generated a broadband excitation. The excitation and the output of the filter were measured by the A/Ds in the time domain. Dozens of repeated experiments yielded identical measurements, except for occasional differences in the least significant bit. Clearly, digitization error dominated. Making the UBBE assumption, with bounds derived from the discrete voltages measurable by the A/Ds, is reasonable for this measurement.

Using bounds to describe measurement error is at least as old as the use of toleranced mechanical drawing. Instrument manufacturer’s specifications often give bounds on measurement error. Smit [1] described a general theory for computing the possible values of quantities derived from measurements under the UBBE assumption. Schweppe [2] showed how to solve a number of parameter and state identification problems under the UBBE assumption. There has been considerable recent work in the controls community on the problem of identifying the parameters

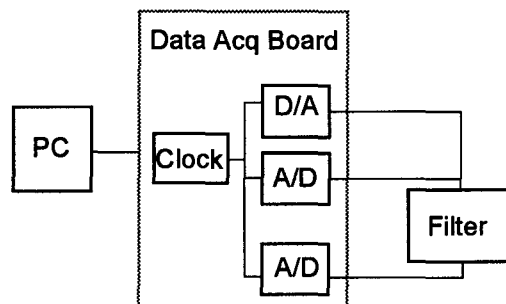


Figure 1. Audio-frequency filter measurement

(or bounds on the parameters) of a linear system from time-domain measurements under the UBBE assumption [4]-[6].

This paper is concerned with identifying the parameters of a single-input, single output, lumped-parameter, linear, time invariant system based on measurements of the complex spectra of a broadband excitation signal and the output of the system (Fig. 2). Schoukens and Pintelon [7] have studied how to perform this identification when the measurement noise is modeled as being random and drawn from some known distribution.

First, this paper formalizes the models of the device under test and measurement uncertainty to be considered. Second, it shows that the set of all possible parameter values is the union of a large number of polyhedral sets. It describes an algorithm for computing a single value for each of the parameters. Last, it presents an example of using the algorithm on measured data.

2 MODELS OF MEASUREMENT UNCERTAINTY AND DEVICE UNDER TEST

Assume that the complex excitation spectrum $\hat{X}(\omega)$ and output spectrum $\hat{Y}(\omega)$ are measured at a discrete set of F frequencies $\Omega = \{\omega_0, \omega_1, \dots, \omega_{F-1}\}$. These measurements can, for example, be performed on a network analyzer. Assume further that for each $\omega \in \Omega$, bounds $\underline{X}(\omega)$, $\bar{X}(\omega)$, $\underline{Y}(\omega)$, and $\bar{Y}(\omega)$ on the true spectra $X(\omega)$, $Y(\omega)$ have been obtained such that¹

$$\text{Re}(\underline{X}(\omega)) \leq \text{Re}(X(\omega)) \leq \text{Re}(\bar{X}(\omega)) \quad (1)$$

$$\text{Im}(\underline{X}(\omega)) \leq \text{Im}(X(\omega)) \leq \text{Im}(\bar{X}(\omega)) \quad (2)$$

$$\text{Re}(\underline{Y}(\omega)) \leq \text{Re}(Y(\omega)) \leq \text{Re}(\bar{Y}(\omega)) \quad (3)$$

$$\text{Im}(\underline{Y}(\omega)) \leq \text{Im}(Y(\omega)) \leq \text{Im}(\bar{Y}(\omega)). \quad (4)$$

The device under test is to be modeled as linear, time invariant, and delay-free with N zeros and M poles. The transfer function of the system is given by

$$\frac{Y(\omega)}{X(\omega)} = H(j\omega) = \left(\sum_{i=0}^N a_i \Theta_i^N(j\omega) \right) / \left(\sum_{i=0}^M b_i \Theta_i^M(j\omega) \right)$$

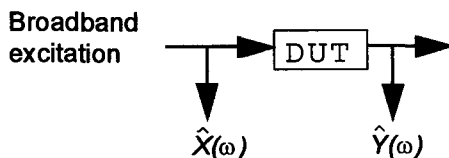


Figure 2. Assumed measurement set-up

1. This formulation, with rectilinear bounding boxes around $X(\omega)$ and $Y(\omega)$, is somewhat arbitrary. It would also be reasonable to consider bounding circles or ellipses, for example.

or, more succinctly,

$$Y(\omega)b^T\Theta^M(j\omega) - X(\omega)a^T\Theta^N(j\omega) = 0 \quad (5)$$

where the parameter vectors $a \in \mathfrak{R}^N$ and $b \in \mathfrak{R}^M$ are to be determined from the measurements and $\Theta^K(x)$ is a vector of functions that form a basis for the polynomials of degree K . Typically $\Theta^K(x)$ is $[1, x, x^2, \dots, x^K]^T$. It could also be the Tschebyshev polynomials, or some other orthogonal polynomials, up to degree K . Normally, one element of a or b is forced to be a chosen constant, to eliminate parameter choices that differ only by a multiplicative constant.

3 THE SET OF FEASIBLE PARAMETERS

In (5), $X(\omega)$ and $Y(\omega)$ are any values that satisfy (1)-(4). Thus, there is a set S of feasible parameter values, namely the set of parameters (a, b) for which there exists $X(\omega)$ and $Y(\omega)$ that satisfy (1)-(5). S is a subset of $\mathfrak{R}^N \times \mathfrak{R}^M$ and a function of $\underline{X}, \bar{X}, \underline{Y}, \bar{Y}, M$ and N .

The set of feasible parameters S gives all possible identifications of the system under the UBBE assumption. If the boundaries of S were easy to compute and could be stored easily, they could be used directly to solve problems such as:

- computing bounds on the possible parameter values,
- finding stable parameters, by searching within S , and
- comparing two measured systems to see if they are the same to within measurement error, by checking whether their respective feasible parameter sets overlap.

Unfortunately, as we will now see, there is a strong indication that it is time-consuming to compute S explicitly.

Theorem 1: S is the union of 2^{N+M} polyhedral sets, each with at most $4F$ facets. (A similar theorem for the time domain setting appears in [6].)

Proof: Suppose (falsely) that we knew the signs of each element of a and b . We show that then S would be the solution set of $4F$ linear inequalities.

Let $r(\omega)$ be the real part of the left-hand side of (5), and $c(\omega)$ the imaginary part:

$$\begin{aligned} r(\omega) = & \sum_i Re[Y(\omega)]b_i Re[\Theta_i^N(j\omega)] - \sum_i Im[Y(\omega)]b_i Im[\Theta_i^N(j\omega)] \\ & - \sum_i Re[X(\omega)]b_i Re[\Theta_i^N(j\omega)] + \sum_i Im[X(\omega)]b_i Im[\Theta_i^N(j\omega)] \end{aligned} \quad (6)$$

(7)

$$c(\omega) = \sum_i \operatorname{Re}[Y(\omega)] b_i \operatorname{Im}[\Theta_i^N(j\omega)] + \sum_i \operatorname{Im}[Y(\omega)] b_i \operatorname{Re}[\Theta_i^N(j\omega)] \\ - \sum_i \operatorname{Re}[X(\omega)] b_i \operatorname{Im}[\Theta_i^N(j\omega)] - \sum_i \operatorname{Im}[X(\omega)] b_i \operatorname{Re}[\Theta_i^N(j\omega)]$$

Equation (5) is equivalent to (8) and (9)

$$r(\omega) = 0 \quad (8)$$

$$c(\omega) = 0. \quad (9)$$

Let

$$Y_R(b, \omega, i) = \begin{cases} \operatorname{Re}[Y(\omega)], & \text{if } b_i \operatorname{Re}[\Theta_i^M(j\omega)] \geq 0 \\ \operatorname{Re}[\bar{Y}(\omega)], & \text{otherwise} \end{cases}$$

$$X_R(a, \omega, i) = \begin{cases} \operatorname{Re}[X(\omega)], & \text{if } a_i \operatorname{Re}[\Theta_i^N(j\omega)] \geq 0 \\ \operatorname{Re}[\bar{X}(\omega)], & \text{otherwise} \end{cases}$$

$$Y_I(a, \omega, i) = \begin{cases} \operatorname{Im}[Y(\omega)], & \text{if } a_i \operatorname{Im}[\Theta_i^N(j\omega)] \geq 0 \\ \operatorname{Im}[\bar{Y}(\omega)], & \text{otherwise} \end{cases}$$

$$Y_I(b, \omega, i) = \begin{cases} \operatorname{Im}[Y(\omega)], & \text{if } b_i \operatorname{Im}[\Theta_i^M(j\omega)] \geq 0 \\ \operatorname{Im}[\bar{Y}(\omega)], & \text{otherwise.} \end{cases}$$

For each ω , (1)-(4) and (8) are equivalent to the following pair inequalities:

(10)

$$\sum_i Y_R(-b, \omega, i) b_i \operatorname{Re}[\Theta_i^N(j\omega)] - \sum_i Y_I(b, \omega, i) b_i \operatorname{Im}[\Theta_i^N(j\omega)] \\ - \sum_i X_R(a, \omega, i) b_i \operatorname{Re}[\Theta_i^N(j\omega)] + \sum_i X_I(-a, \omega, i) b_i \operatorname{Im}[\Theta_i^N(j\omega)] \geq 0$$

(11)

$$\sum_i Y_R(b, \omega, i) b_i \operatorname{Re}[\Theta_i^N(j\omega)] - \sum_i Y_I(-b, \omega, i) b_i \operatorname{Im}[\Theta_i^N(j\omega)] \\ - \sum_i X_R(-a, \omega, i) b_i \operatorname{Re}[\Theta_i^N(j\omega)] + \sum_i X_I(a, \omega, i) b_i \operatorname{Im}[\Theta_i^N(j\omega)] \leq 0$$

Equations (1)-(4) and (9) are equivalent to a similar pair of inequalities. Both pairs of inequalities are linear, since $\Theta_i^M(j\omega)$, $\Theta_i^N(j\omega)$, X_R , X_I , Y_R , and Y_I are constant for fixed ω .

When the signs of the elements of a and b are fixed, S is the solution set of $4F$ linear inequalities. Then S is a polyhedral set with at most $4F$ facets. But the signs of a and b are in fact unknown. So S is the union of such polyhedral sets, where the union is taken over all of the choices of signs for the elements of a and b . There are 2^{N+M} such choices of sign. \square

Theorem 1 suggests that computing S explicitly will take vast amounts of computer time, due to the exponential growth of the number of polyhedra in S as N and M increase. Points within a particular polyhedron, however, can be found quickly by linear programming.

4 FINDING A SINGLE SOLUTION

Because of the apparent difficulty of computing S explicitly, the remainder of this paper is concerned with the simpler problem of finding a single feasible parameter $(a, b) \in S$. This section shows how this problem is transformed into a nonlinear optimization problem that is solvable with commercially available code.

This is done by finding not only values for a and b , but also corresponding values for $X(\omega)$ and $Y(\omega)$ at the same time. This could be done by solving (1)-(5) with a solver for nonlinear equations under box constraints. On some occasions, (1)-(5) will have no solution (usually because N or M is too small). When this happens, a numerical nonlinear equation solver will fail to converge. When nonconvergence occurs it is impossible to determine whether (1)-(5) in fact have no solution or if nonconvergence is due to numerical errors. There are nonlinear equation solvers based on interval arithmetic that will either provide tight lower and upper bounds on a solution or verify that no solution exists [8]. However, the computing time required by such exact solvers increases exponentially with the number of variables in the problem.

In order to make the numerical solver converge, even in the case where (1)-(5) have no solution, we introduce a new positive real variable e . This e is an upper bound on the absolute error in the constraint equations (8) and (9):

$$|r(\omega)| \leq e \quad (12)$$

$$|c(\omega)| \leq e. \quad (13)$$

e can be set to a large enough value that (12) and (13) are satisfied, whatever initial values that satisfy (1)-(4) are chosen for a , b , $X(\omega)$ and $Y(\omega)$. e is then minimized using a numerical optimization code. A well-designed code should always converge, since e is bounded below by 0. If e can be reduced almost to zero¹ while maintaining values for a , b , $X(\omega)$ and $Y(\omega)$ that satisfy (1)-(4), (12), and (13), then a solution to (1)-(5) is given by the final values of a and b . If e cannot be reduced to zero, that suggests that (1)-(5) have no solution and that N or M should be increased.

1. e cannot, of course, be reduced exactly to zero because of the numerical round-off errors in floating point computations.

Specifically, the following constrained, nonlinear optimization problem in real variables is formed and solved numerically: *Find the real $(M + N + 4F + 1)$ -vector $(a, b, Re[X(\omega)], Im[X(\omega)], Re[Y(\omega)], Im[Y(\omega)], e)$ that minimizes e such that (1)-(4) hold and $e \geq 0$, $r(\omega) \leq e$, $-r(\omega) \leq e$, $c(\omega) \leq e$ and $-c(\omega) \leq e$, and $b_0 = 1$.*

This optimization problem is solved using the iterative, constrained, nonlinear optimization routine *constr* from the Matlab Optimization Toolbox. Following a recommendation in [9], Forsythe polynomials [10] are used for the polynomial basis $\Theta^K(x)$ to improve the numerical stability of the optimization code.

To start the iterative code, $X(\omega)$ is set equal to $(\underline{X}(\omega) + \bar{X}(\omega))/2$ and $Y(\omega)$ is set equal to $(\underline{Y}(\omega) + \bar{Y}(\omega))/2$. Then the initial values for a and b are set to those that give the least squares fit to $X(\omega)$ and $Y(\omega)$, and e is set large enough to satisfy (12) and (13).

5 EXAMPLE

The algorithm of the previous section was applied to measurements of a passive bandpass filter from [11]. The excitation was a 16-frequency multisine in the band 244.1Hz to 976.6 Hz. An 8-bit digitizer was used to measure the time-domain signals. The measurement was repeated 25 times.

The bounds $\underline{X}(\omega)$, $\bar{X}(\omega)$, $\underline{Y}(\omega)$, and $\bar{Y}(\omega)$ were taken to be the extremal values encountered among the 25 measurements. For example, for each ω , $Re[\underline{X}(\omega)]$ was taken to be the smallest measured value $Re[\hat{X}(\omega)]$ from among the 25 measurements.

The optimization required five iterations. The final value of the maximum absolute equation error was $e = 1.5951 \cdot 10^{-20}$, which is well within round-off error of zero.

Fig. 3 shows the amplitude and phase of the non-parametric transfer function $\hat{Y}(\omega)/\hat{X}(\omega)$ of all 25 measurements (each measured value is indicated with a “+”) and the identified parametric transfer function $H(j\omega)$. Fig. 4 shows the real and imaginary parts of same data.

Figs. 5-8 illustrate that the algorithm results in values for $X(\omega)$ and $Y(\omega)$ that satisfy (1)-(4). Fig. 5 shows the differences $Re[\underline{X}(\omega) - X(\omega)]$ and $Re[\bar{X}(\omega) - X(\omega)]$. Since the values of $Re[\underline{X}(\omega) - X(\omega)]$ are below or on the x-axis, and the values of $Re[\bar{X}(\omega) - X(\omega)]$ are above or on the x-axis, (1) is satisfied. Fig. 6 shows $Im[\underline{X}(\omega) - X(\omega)]$ and $Im[\bar{X}(\omega) - X(\omega)]$ in the same manner, illustrating that (2) is satisfied. Similarly, Fig. 7 shows that (3) is satisfied and Fig. 8 shows that (4) is satisfied.....

Several of the differences plotted in Figs. 5-9 appear to be on the x-axis, indicating that the corresponding constraint was satisfied at equality. The smallest difference was $1.2 \cdot 10^{-9}$, numerically equal to zero. The numerical method found parameter values on the border of S .

The signs of the elements of a and b did not change from those of their initial values.

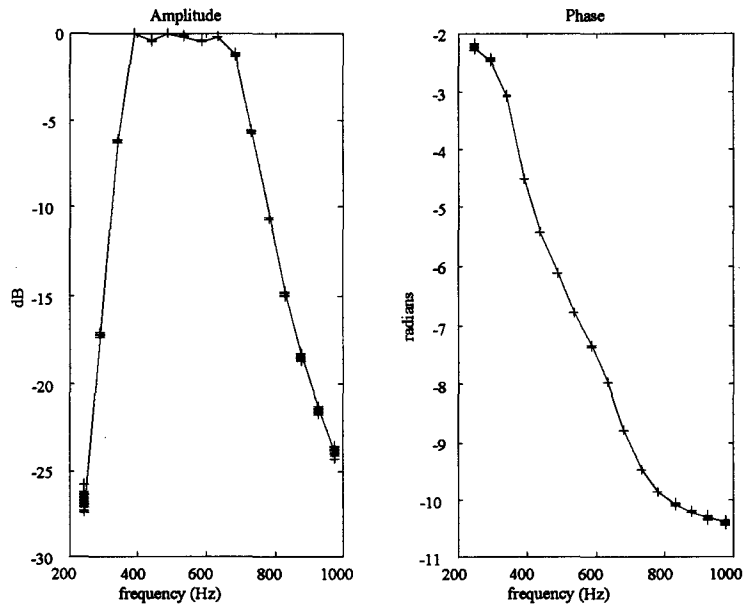


Figure 3. Amplitude and phase of nonparametric transfer function (measured datum = "+") and identified transfer function

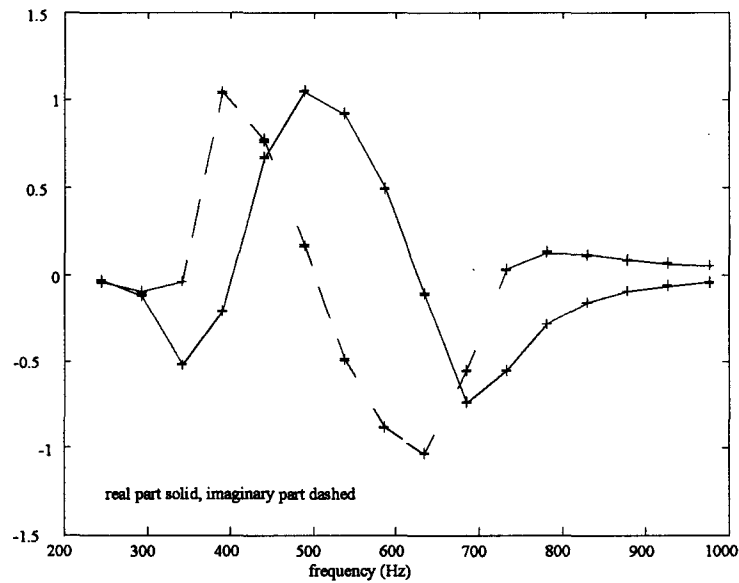


Figure 4. Real and imaginary parts of nonparametric transfer function

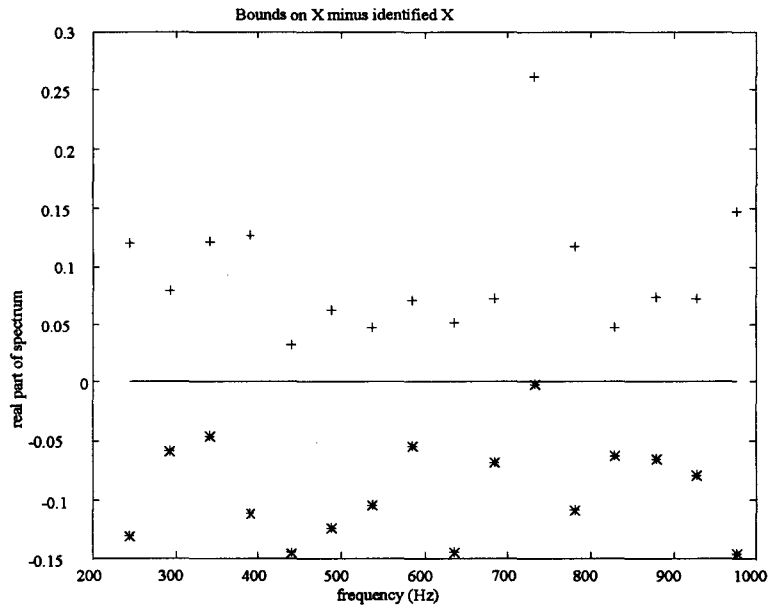


Figure 5. Difference between real parts of bounds on X and identified X . $Re[\underline{X}(\omega) - X(\omega)]$ appears as "*", $Re[\bar{X}(\omega) - X(\omega)]$ as "+"

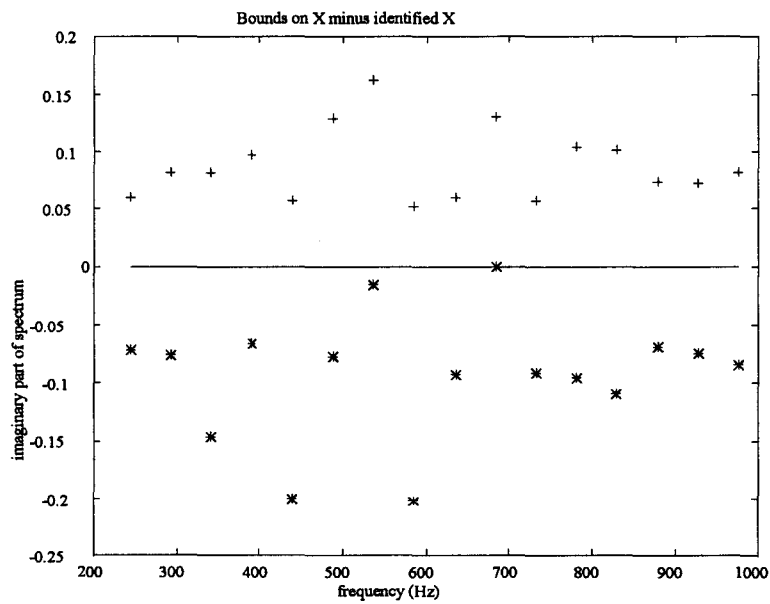


Figure 6. Difference between imaginary parts of bounds on X and identified X . $Im[\underline{X}(\omega) - X(\omega)]$ appears as "*", $Im[\bar{X}(\omega) - X(\omega)]$ as "+".

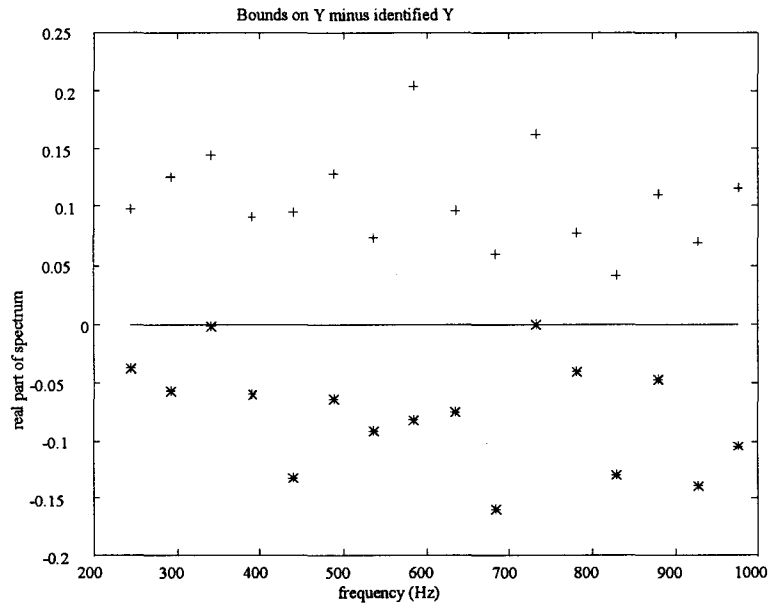


Figure 7. Difference between real parts of bounds on Y and identified Y.
 $Re[\underline{Y}(\omega) - Y(\omega)]$ appears as "*", $Re[\bar{Y}(\omega) - Y(\omega)]$ as "+"

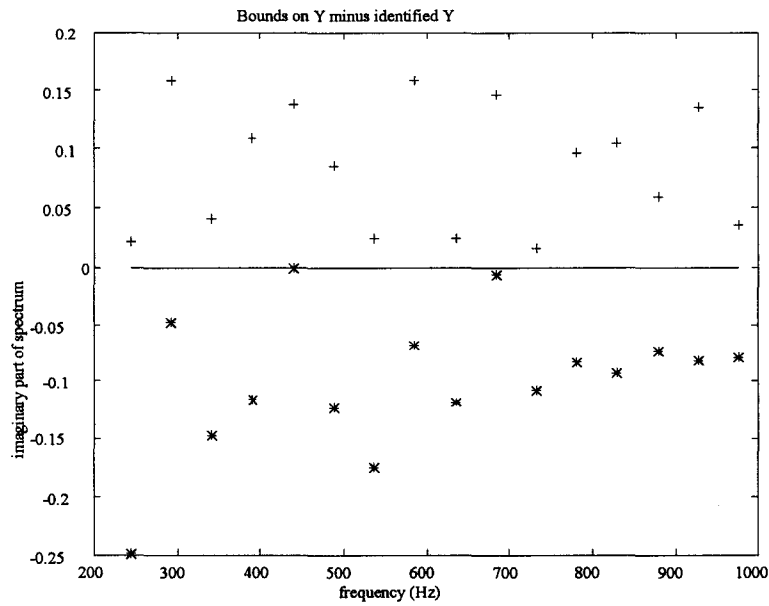


Figure 8. Difference between imaginary parts of bounds on Y and identified Y.
 $Im[\underline{Y}(\omega) - Y(\omega)]$ appears as "*", $Im[\bar{Y}(\omega) - Y(\omega)]$ as "+".

6 CONCLUSIONS

This paper contains two main contributions. First, it shows that the set of feasible parameter values is the union of polyhedra, where the number of polyhedra grows exponentially as the number of parameters increases. This exponential growth suggests that computing the set of all possible parameter values would be computationally infeasible. Second, it demonstrates how a commercially available optimization code can be used to find a single feasible value for each parameter.

Finding a single value for each parameter in the example took only five iterations of a numerical solver, starting from the least squares solution. The signs of the parameters didn't change from those of their initial values. Similar behavior was noted on other data sets. This suggests that the parameter values computed by least squares often have signs that yield a polyhedron that is non-empty. A possible direction for future research would be to investigate how well S is approximated by the union of a small number of polyhedra near the least squares fit.

ACKNOWLEDGMENTS

Thanks go to Yves Rolain for many informative discussions on system identification topics over the years and for introducing me to Forsythe polynomials, and to Ron Van Iwaarden for an interesting discussion on the potential benefits and problems with using interval arithmetic-based, guaranteed nonlinear equation solvers. Kirsten Nelson suggested many improvements to the readability of this paper and permitted several late nights to be spent at the office. David Smith and Nick Tufillaro proofread and suggested improvements. The author would also like to thank Wes Higaki, Randy Coverstone, and Bill Shreve for providing for management support.

REFERENCES

- [1] M. K. Smit, "A novel approach to the solution of indirect measurement problems with minimal error propagation," *Measurement* 1(4), p. 181-190, 1983.
- [2] F. C. Schweppe, *Uncertain Dynamical Systems*, Prentice-Hall, Englewood Cliffs, NJ, 1973.
- [3] *Guide to the Expression of Uncertainty in Measurement*, International Standards Organization, 1993.
- [4] M. Milanese and A. Vicino, "Optimal estimation theory for dynamic systems with set membership uncertainty: an overview" in Mario Milanese, et al., eds., *Bounding Approaches to System Identification*, New York: Plenum, 1996.
- [5] E. Walter and H. Piet-Lahanier, "Recursive robust minimax estimation," in Mario Milanese, et al., eds., *Bounding Approaches to System Identification*, New York: Plenum, 1996.
- [6] Y. A. Merkurjev, "Identification of linear objects with bounded disturbances in both input and output channels", in Mario Milanese, et al., eds., *Bounding Approaches to System Identification*, New York: Plenum, 1996.
- [7] J. Schoukens and R. Pintelon, *Identification of Linear Systems: A Practical Guide to Accurate Modeling*, Pergamon, 1991.

- [8] R. Hammer, M. Hocks, et al., *Numerical Toolbox for Verified Computing I: Basic Numerical Problems*, New York: Springer-Verlag, 1993.
- [9] Y. Rolain, G. Vandersteen, D. Schreurs, S. Van den Bosch, "Parametric modeling of linear time invariant S-parameter devices in the Laplace domain," Proc. of the IEEE Instrumentation and Measurement Technology Conference, Brussels, Belgium, pp. 1244-1249, June 4-6, 1996.
- [10] G. E. Forsythe, "Generation and Use of Orthogonal Polynomials for Data-Fitting with a Digital Computer," *Journal of the Society for Industrial Applied Mathematics*, 5(3), pp. 74-88, 1957.
- [11] I. Kollár, *Frequency Domain System Identification Toolbox*, Natick, MA: MathWorks, p. A12, 1994.